

Experimental and analytical study of the effect of variable amplitude loadings in VHCF regime

T. Müller, M. Sander*

Institute of Structural Mechanics, University of Rostock, 18059 Rostock, Germany

* Corresponding author: manuela.sander@uni-rostock.de

Abstract

Components and structures (e.g. helicopter rotors, wind turbine components or wheelset axels) are commonly exposed a very high number of cycles with variable amplitudes. For the study of the influence of variable amplitude loadings in the very high cycle fatigue regime different load-time-histories up to 10^9 cycles are used, which have different amounts of small amplitudes beneath the fatigue strength of the investigated material. The experiments are performed with an ultrasonic fatigue testing system with frequencies up to 21 kHz. In order to avoid an excessive heat development of the specimen, pulsed loadings with adequate pause lengths are applied. Therefore, only block loadings can be realized. The used load-time-histories have been counted by the rainflow method and then divided into different number of classes providing that within every class a minimum number of cycles restricted by the experimental performance is given. The classes have been reconstructed to a load-time-history by varying the sequence of the classes. The influence of the different reconstructions as well as of the amount of the amplitudes beneath the fatigue strength is quantified by the fatigue lifetime. These experimental data are used to proof conventional analytical approaches (*Palmgren-Miner's rule*) of structural durability in the VHCF regime.

Keywords very high cycle fatigue, variable amplitude loading, fatigue life prediction, load interaction effect, short crack growth

1. Introduction

In technical constructions of different application fields, components are very often subjected to cyclic stresses. Components like drive shafts, gear shafts, wheelset axles, helicopter rotors or highly stressed engine parts, such as blades, are often cyclically loaded with more than 10^7 cycles up to 10^9 and more cycles. The high number of load cycles can be attributed to a very long period of service up to 30 years or to high service frequencies. In present fatigue design standards the influence and effect of such high number of load cycles on the fatigue behavior are not sufficiently taken into account.

As *Bathias* [1] already showed in 1999, the determined fatigue strength, defined by the early investigations of *Wöhler*, does not exist. Thus, a decrease of the S-N curve is observable in the very high cycle fatigue regime, as numerous studies (e.g. [2-5]) have shown. The decrease in fatigue strength is caused by the transition from surface to subsurface crack initiation [5-7]. Moreover, microstructural features like cavities, non-metallic inclusions, grain boundaries, porosities or oxide layers at the surface and inside a component could lead to crack initiation.

Cracks, initiated at non-metallic inclusions, usually show the typical formation of a fish-eye. In the vicinity of inclusions within the fish-eye a distinctive area could be observed [8-10]. *Murakami* calls it an optical dark area (ODA) with a more rough fracture surface in comparison to the remaining fish-eye fracture surface. He assumed that the area occur due to hydrogen accumulation during cyclic loading. He also proposes a relationship between the size of the ODAs and non-metallic inclusions as well as the number of cycles to failure.

However, the influence of variable amplitude loading (VAL) on the fatigue behavior in the VHCF regime is, despite a few studies [11-18], poorly investigated. For instance *Mayer* [12] showed with two-step loading tests that low load amplitudes beneath the fatigue strength contribute to fatigue

damage depending on the height of the maximum load amplitudes.

2. Material and experimental procedure

2.1. Material

The experimental investigations are performed with specimens with a minimum diameter of 4 mm shown in Fig. 1. All specimens were machined from a 20 mm round bar of the quenched and tempered high-strength steel 34CrNiMo6. The chemical composition of the steel is summarized in Table 1 and the static material parameters are shown in Table 2.

Table 1. Chemical composition of the investigated high-strength steel (in wt %)

C	Si	Mn	Cr	Mo	Ni
0.34	0.3	0.5	1.5	0.2	1.5

Table 2. Mechanical Properties

UTS [MPa]	YS [MPa]	Young's modulus [GPa]	Breaking elongation [%]
1200	1000	210	9

An average Vickers hardness of the material was 350 HV. The surface of the specimen has been emery-polished after machining.

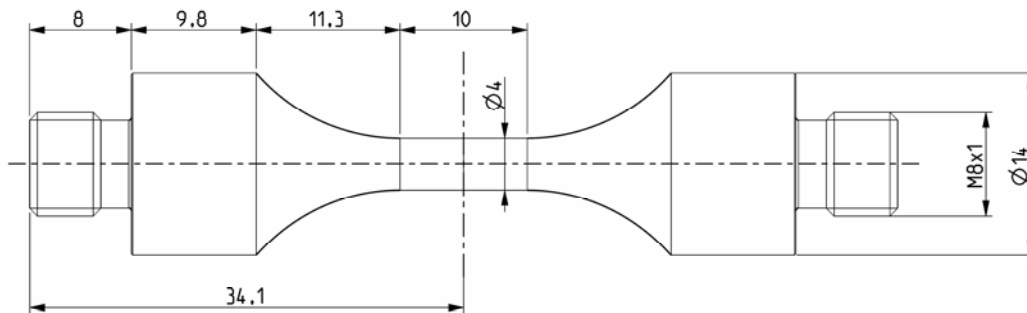


Figure 1. Specimen

2.2. Ultrasonic fatigue testing system

In service, components and structures are rather subjected to variable amplitude loadings (VAL) than to constant amplitude loadings (CAL). Fatigue tests with variable amplitude loadings or load time histories in the regime of 10^9 cycles or even higher are too time consuming and expensive using conventional testing systems. Therefore, an ultrasonic fatigue testing system of the BOKU

Vienna [19] is used. The system is stimulating the specimen in its resonance frequency and is with about 21 kHz many times higher than loading frequencies of conventional systems. Tests have been performed in pulse-pause-sequences to avoid excessive heating of the specimen. Thus, experiments with a fatigue life up to 10^9 cycles take between 0.6 and 6 days depending on the pulse- and pause-sequence. Using the ultrasonic fatigue testing technique no load time history could be subjected to the specimen. Because of increasing vibration amplitudes at the beginning and decreasing amplitudes at the end of a pulse, only block loading tests can be realized. Thus, for systematic studies firstly two block loading tests are performed with different block loading length. Furthermore, a reconstruction algorithm, generating adequate cumulative frequency distributions of load cycles, is used to perform fatigue tests on the basis of a load time history. Therefore, the software Ultrasonic Fatigue Testing Software for Variable Amplitude Loading (UFaTeS^{VAL}), which has been developed at the Institute of Structural Mechanics at the University of Rostock, is used for data acquisition and controlling of the VAL experiments.

2.3. Variable amplitude loading tests

A high demand is requested for investigating the influence of variable amplitude loadings, and load interaction effects in particular, on short crack growth and crack initiation in the VHCF.

2.3.1. Two-step loading tests

For systematic studies of the influence of load interaction effects on the fatigue life, particularly with regard to short crack growth, two-step loading tests have been performed (Fig. 2). The amount of numbers n_1 of the maximum load amplitude of the cumulative distribution is 10.000 cycles and constant for all experiments. Tests have been carried out with different maximum load amplitudes with 110% and 120% of the fatigue strength σ_D for each experiment. The low block load is 90% of the fatigue strength and the number of cycles n_2 was varied, characterized by the ratio $R_{bl} = n_2/n_1$. Three different ratios of 1, 10 and 100 have been investigated. However, the ratio was kept constant within one test. The two blocks are repeated until the specimen fails or the limit of 10^9 cycles is reached.

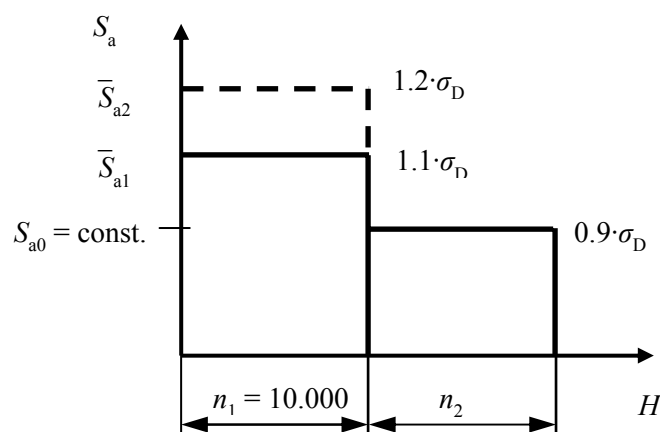


Figure 2. Schematic procedure of two-step loading tests

2.3.1. Tests with load-time history FELIX

For the investigation of realistic variable amplitude loadings, the standardized helicopter load spectrum FELIX [20] has been used. Therefore, the stress amplitudes of the FELIX spectrum have been transformed to a constant R -ratio of -1 using the equations accounting for the mean stress effect. After dividing the spectrum into different classes, they have been reconstructed to different load sequences (Fig. 3). The load sequence FELIX 10 was reconstructed with decreasing load amplitudes starting with the maximum amplitude and ending with the lowest amplitude. The load sequence FELIX 11 starts with the lowest amplitude and is step-wise increased up to the maximum load amplitude. The load amplitudes of the last reconstructed sequence FELIX 12 is randomly mixed. Each sequence is repeated until failure occurs or the limit of 10^9 cycles is reached.

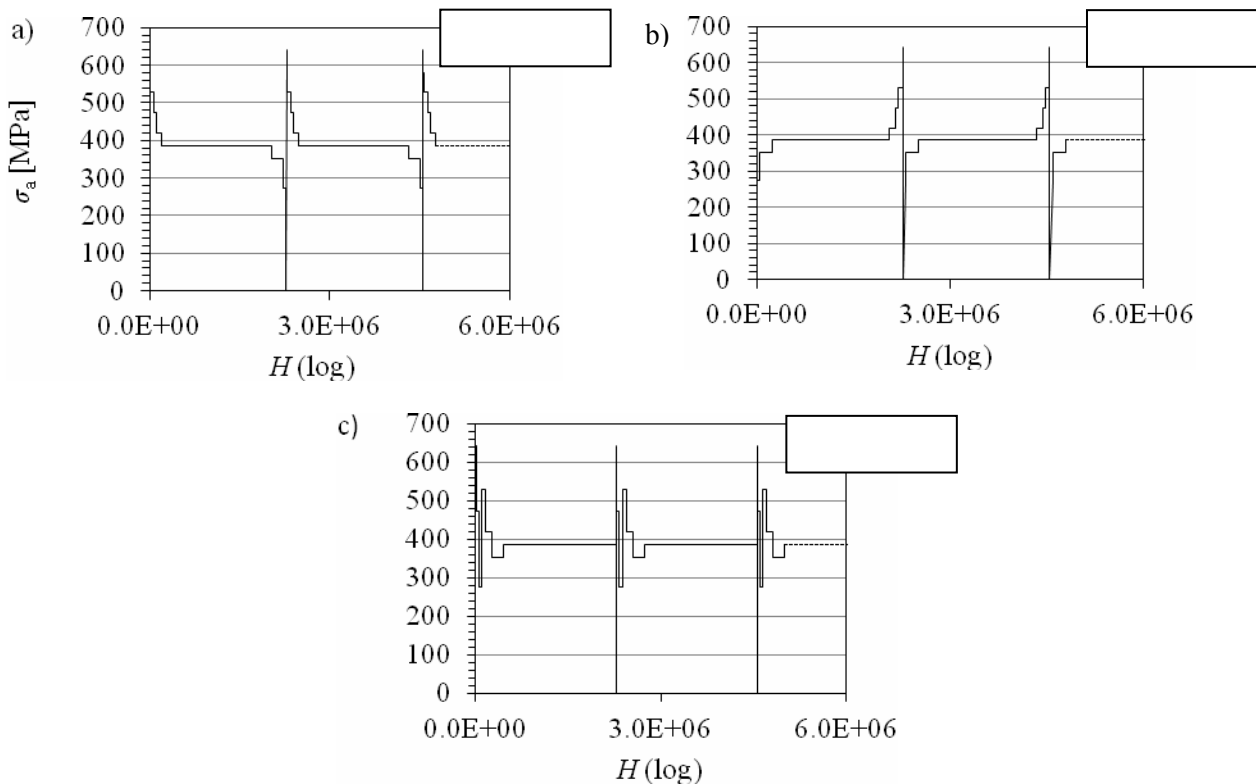


Figure 3. Reconstructed load time history FELIX with a) decreasing load amplitudes, b) increasing load amplitudes and c) mixed load amplitudes

3. Results

The influence of the size of non-metallic inclusions on the number of cycles to failure is shown in Figure 4, where $area_{inc}$ is the inclusion size projected on the plane perpendicular to the maximum principal stress. The data of constant amplitude (CA) loading tests show no significant influence of the inclusion size on the lifetime. In contrast, the size of inclusions tends to decrease with increasing lifetime for all variable amplitude (VA) loading tests.

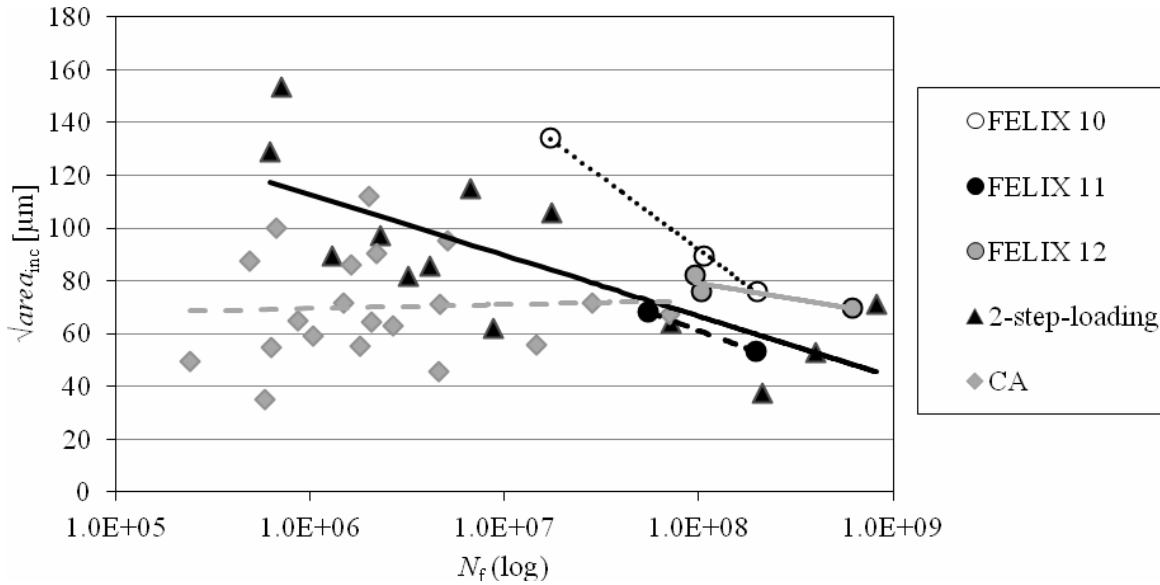


Figure 4. Influence of inclusion size on the fatigue life

Fig. 5 shows the results of the modified S-N curves of the VA-tests (FELIX) in comparison to the tests with constant amplitude loading using the approach by *Murakami* [8] with

$$\sigma_w = \frac{1.43 \cdot (H_v + 120)}{(\sqrt{\text{area}_{\text{inc}}})^{1/6}} \cdot \left[\frac{1-R}{2} \right]^\alpha \quad (1),$$

for inclusions near to the specimen's surface and

$$\sigma_w = \frac{1.56 \cdot (H_v + 120)}{(\sqrt{\text{area}_{\text{inc}}})^{1/6}} \cdot \left[\frac{1-R}{2} \right]^\alpha \quad (2)$$

for subsurface inclusions.

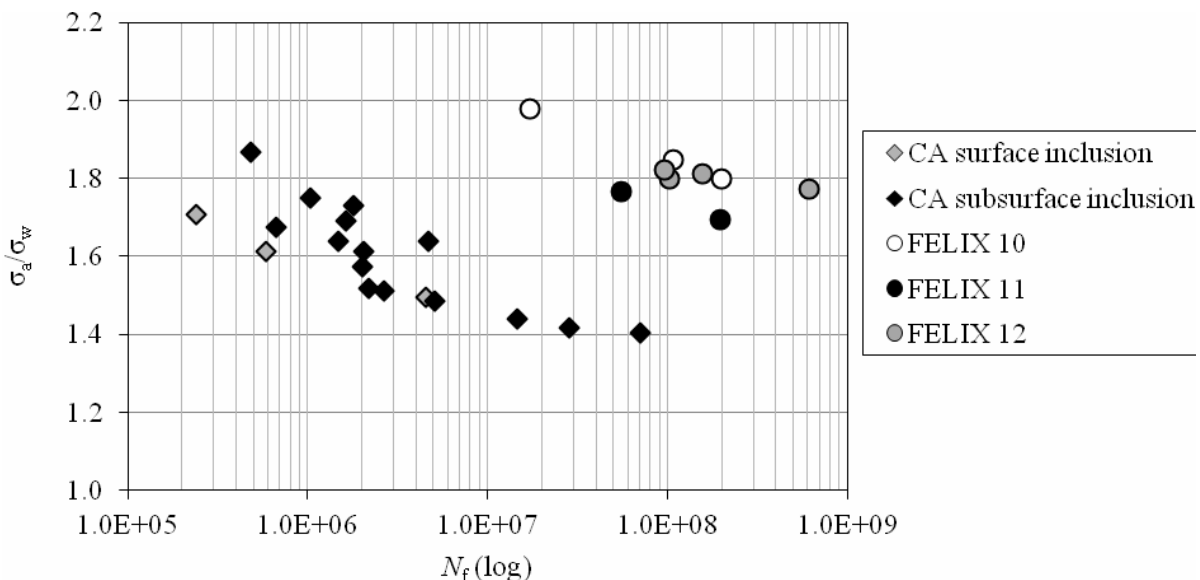


Figure 5. Reconstructed load-time history tests (FELIX) in comparison to constant amplitude tests

The S-N curves are shifted to higher lifetimes for variable amplitude loadings in comparison to constant amplitude loadings. However, the order of load amplitudes influences the lifetime. The reconstructed load time history FELIX 10 with decreasing load amplitudes and the load time history

FELIX 12 with mixed load amplitudes tend to equal lifetimes. Otherwise, the reconstructed load time history FELIX 11 with increasing load amplitudes tends to result in lower lifetimes than FELIX 10 and FELIX 12.

The analyses of the fracture surfaces show circular arrest marks formed around non-metallic inclusions within the fish-eye (Fig. 6b-d) for variable amplitude loading in contrast to the fracture surfaces of specimens subjected to constant amplitude loading (Fig. 6a). This could be an indicator for load interaction effects on the crack growth within the fish-eye, as it is well known in the regime for long crack growth. The arrest marks of FELIX 11 (Fig. 6c) are obviously more pronounced than in the case of FELIX 10 (Fig. 6b) and FELIX 12 (Fig. 6d). However, the sizes of the area, where arrest marks occur, as well as the spacings of the arrest marks are different for the investigated VAL.

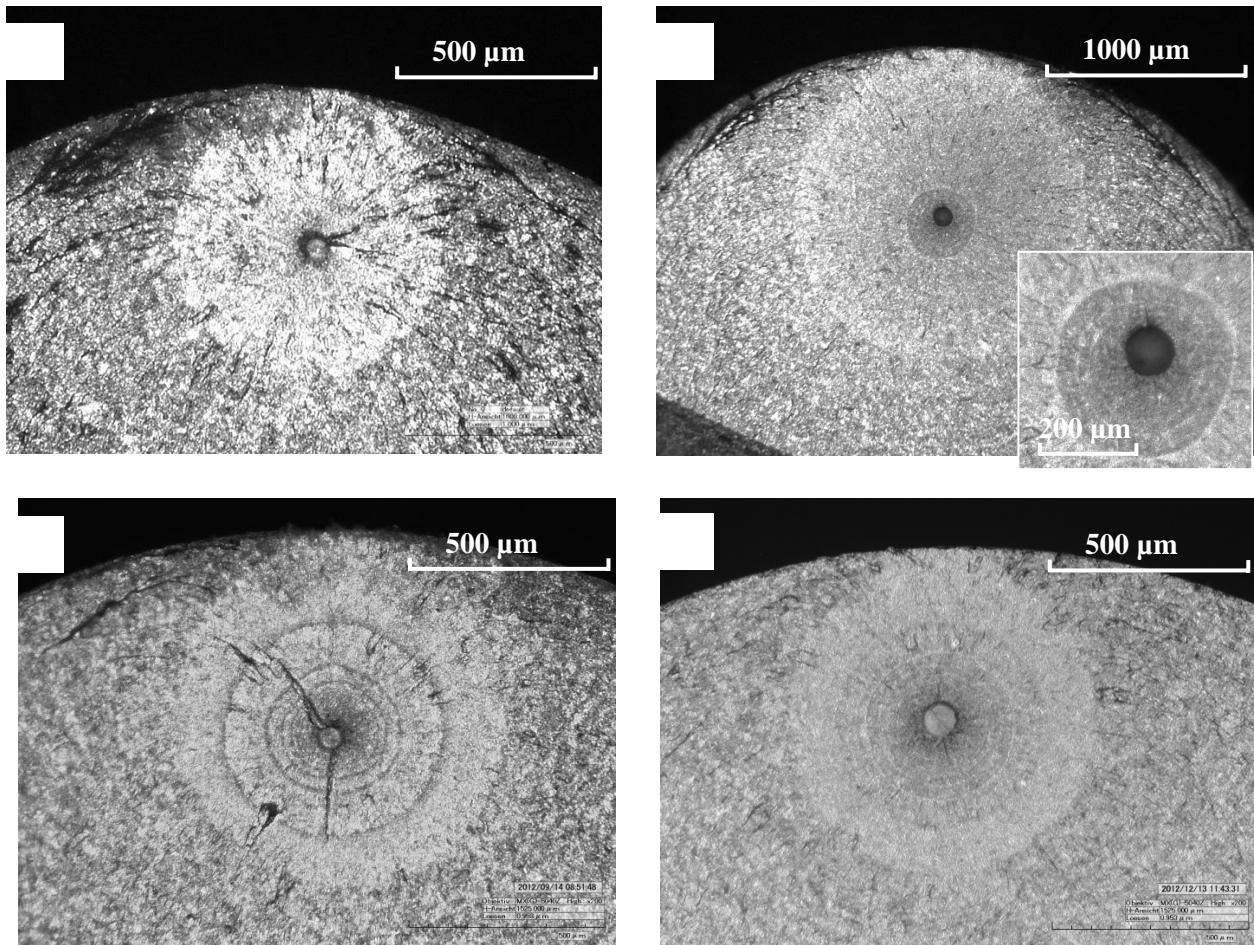


Figure 6. Fracture surfaces with typical fish-eye fracture around non-metallic inclusions: a) constant amplitude loading and FELIX-tests with arrest marks within fish-eye for b) FELIX 10, c) FELIX 11 and d) FELIX 12

By counting and measuring the arrest marks an average crack growth rate da/dN for the crack propagation within the fish-eye can be calculated, as plotted in Fig. 7. By using the \sqrt{area} -approach [8], the stress intensity factor ΔK was determined. Therefore, the stress amplitude of 386 MPa with the highest amount of cycles within the load sequence has been used. The load sequences of FELIX 10 and FELIX 12 lead to similar crack growth rates. In comparison, the crack growth rate of FELIX 11 is shifted to higher crack growth rates. Nevertheless, all three investigated load sequences lead to crack growth rates beneath the threshold value ΔK_{th} for long crack growth.

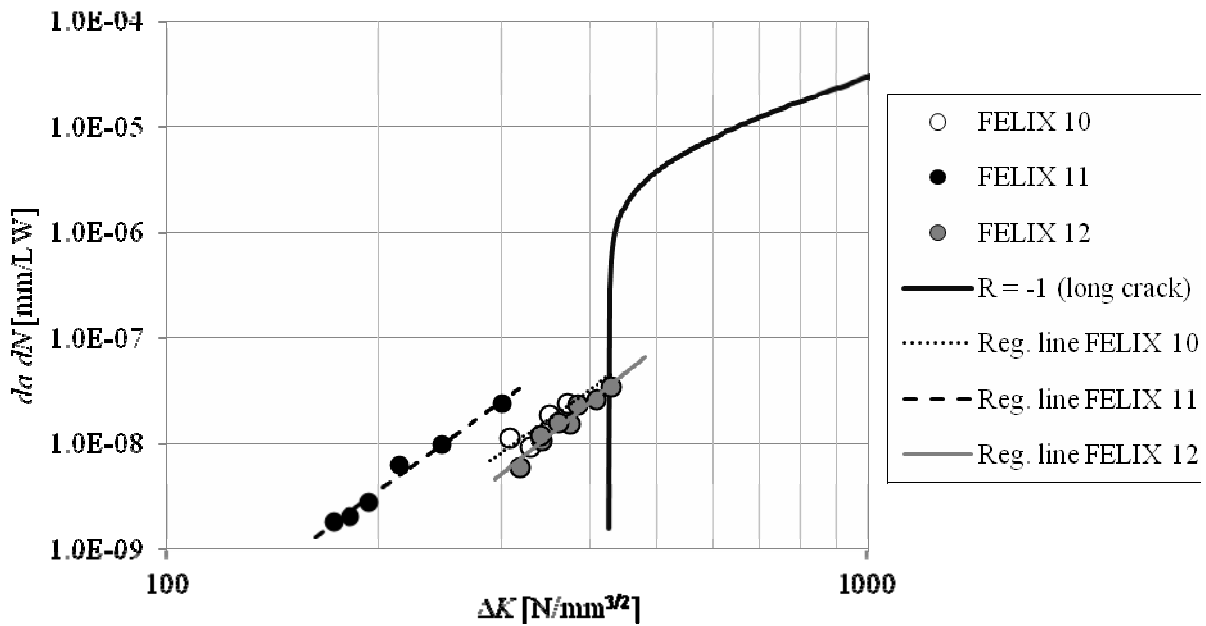


Figure 7. Crack growth curve in comparison to experimentally evaluated crack growth rates with variable amplitude loading tests (FELIX)

Using the *Palmgren-Miner's* rule a fatigue life $N_{f,calc}$ with an assumed damage sum of 1 can be calculated for the investigated variable amplitude loadings (see chap. 2.3). Beside the original *Palmgren-Miner* (PM) approach, the modified and elementary *Palmgren-Miner* approach as well as the approach by *Liu/Zenner* have been taken into account in order to consider amplitude levels beneath the fatigue strength. The calculated fatigue lives $N_{f,calc}$ of the two-step loadings are compared with the appropriate experimental mean fatigue lives $N_{f,exp}$ (Fig. 8). Moreover, in Fig. 8 the scatter bands $N_{f,calc}/N_{f,exp}$ for 10% and 90% probability of survival based on the CA tests are given.

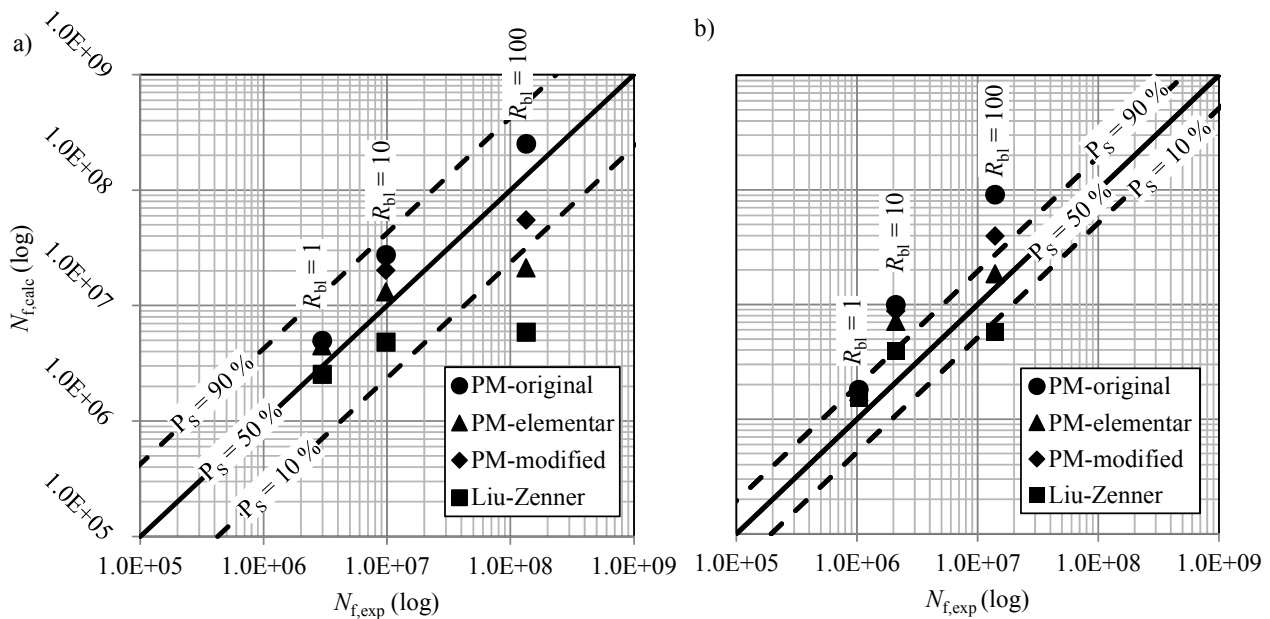


Figure 8. Comparison of two-step loading tests a) $\bar{S}_a = 584$ MPa ($1.1 \cdot \sigma_D$) and b) $\bar{S}_a = 637$ MPa ($1.2 \cdot \sigma_D$) with calculated lifetimes using *Palmgren-Miner's* rule with a damage sum of 1

For $\bar{S}_a = 1.1 \cdot \sigma_D$ (Fig. 8a), the calculated lifetimes for the R_{bl} ratios 1 and 10 are within the scatter band. For $R_{bl} = 100$ only the results of the original and modified *Palmgren-Miner's* rule are within the scatter band. The approach by *Liu/Zenner* always provides the most conservative results, which strongly increase with increasing R_{bl} -ratio.

In comparison, for $\bar{S}_a = 1.2 \cdot \sigma_D$ (Fig. 8b), all approaches provide approximately the same results for the lowest ratio $R_{bl} = 1$. The higher the R_{bl} -ratio is, the more the original PM approach overestimates the lifetime and the values are outside the scatter band. Thus, the low load amplitudes contribute to fatigue damage, if the high block loading is high enough with respect to the lower amplitudes and if the high blocks occur less frequently. The lifetimes obtained by *Liu/Zenner* for the R_{bl} -ratios of 1 and 10 provide good results. At a ratio of 100 it is again conservative. None of the approaches give suitable results for all three R_{bl} -ratios.

In Fig. 9 the calculated fatigue life $N_{f,calc}$ for the investigated load-time history FELIX is compared with the experimental mean fatigue life $N_{f,exp}$ of the three different reconstructed load sequences. For the investigated load sequences FELIX 11 and FELIX 12 the original *Palmgren-Miner's* rule provides results within the scatter band. The approach slightly overestimates the fatigue life of FELIX 10. The elementary *Palmgren-Miner's* rule as well as the approach by *Liu/Zenner* for FELIX 10 and FELIX 11 lead to conservative results, where again the approach by *Liu/Zenner* is the most conservative one. However, it is observable that each approach leads to the same calculated lifetimes $N_{f,calc}$ independent of the used reconstructed load sequence, while the experimental lifetimes $N_{f,exp}$ clearly differ.

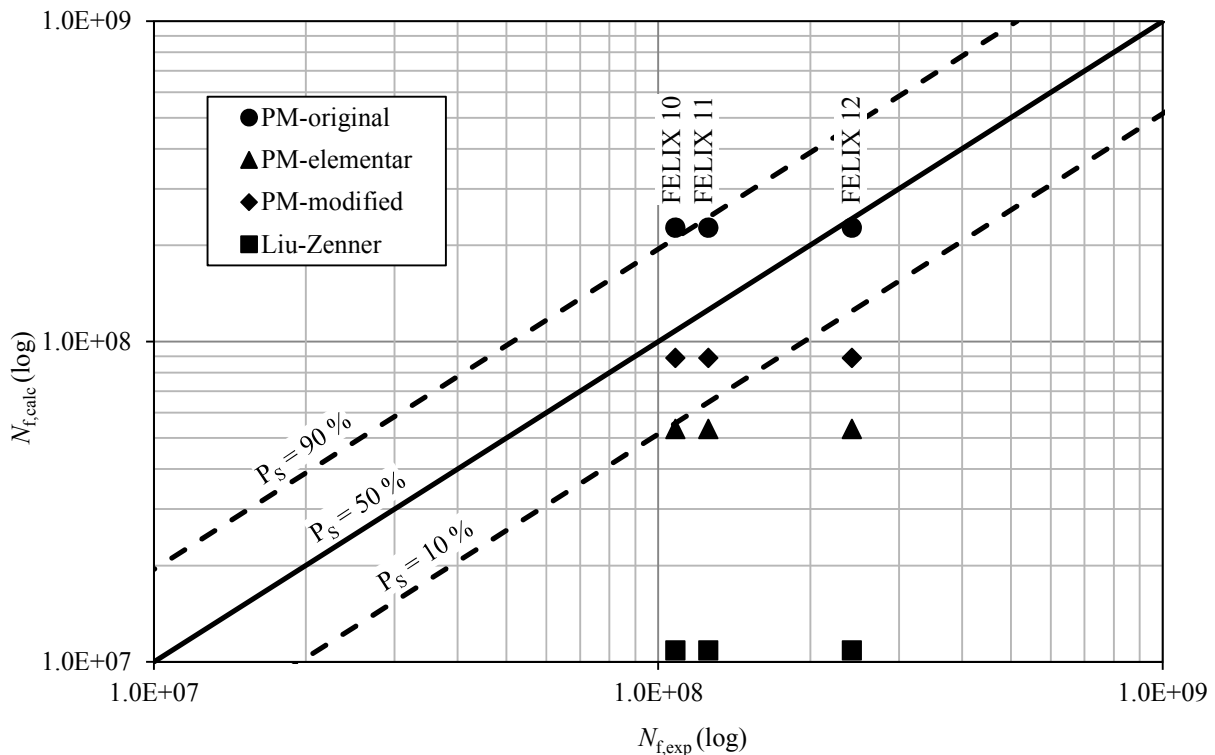


Figure 9. Comparison of different reconstructed load sequences (FELIX) with calculated fatigue life using *Palmgren-Miner's* rule with a damage sum of 1

4. Conclusions

The high strength steel 34CrNiMo6 was investigated in the very high cycle fatigue regime under constant and variable amplitude loadings. An ultrasonic fatigue testing system has been used to perform fatigue tests in adequate testing time. An own developed software UFaTeS^{VAL} was used to realize variable amplitude loading tests. Two-step load amplitudes and reconstructed load time histories were investigated. The main conclusions are as follows:

- (1) The fatigue life of variable amplitude tests is influenced by the size of non-metallic inclusions, in contrast to constant amplitude loadings.
- (2) The two-step loading tests show that load amplitudes below the fatigue strength can contribute to damage depending on the height of the maximum load amplitude and the amount of maximum load amplitudes.
- (3) Variable amplitude loading can provoke the occurrence of arrest marks around non-metallic inclusions within fish-eyes, which are used to calculate a mean fatigue crack growth rate in the fish-eye.
- (4) As the FELIX investigations show, an influence of the kind of reconstruction of the load-time is observable.

Acknowledgements

The authors gratefully acknowledge the financial support by the ‘Deutsche Forschungsgemeinschaft’ (DFG) in the framework of SPP 1466.

References

- [1] Bathias, C.: There is no infinite fatigue life in metallic materials. In: *Fatigue Fract Engng Mat Struct* 1999; 22(7): pp. 559-65
- [2] Marin, I.; Dominguez, G.; Baudry, G.; Vittori, J.F.; Rathery, pp.; Doucet, J.P. et al.: Ultrasonic fatigue tests on bearing steel AISI-SAE 52100 at frequency of 20 and 30 kHz. In: *Int. J. Fatigue* 2003; 25: pp. 1037-1046.
- [3] Pyttel, B.; Schwerdt, D.; Berger, C.: Very high cycle fatigue - Is there a fatigue limit? In: *Int. J. Fatigue* 2011; 33: pp. 49-58
- [4] Sakai, T.: Review and prospects for current studies on very high cycle fatigue of metallic materials for machine structural use. In: *J. Solid Mech Mater Eng* 2009; 3(3): pp. 425-439.
- [5] Shiozawa, K.; Lu, L.; Ishihara, S.: S-N curve characteristics and subsurface crack initiation behavior in ultra-long life fatigue of a high carbon-chromium bearing steel. *Fatigue Fract Engng Mat Struct* 2001; 24(12): pp. 781-90
- [6] Tanaka, K.; Akinawa, Y.: Fatigue crack propagation behavior derived from S-N data in very high cycle regime. *Fatigue Fract Engng Mat Struct* 2002; 25: pp. 775-84
- [7] Ochi, Y.; Matsumura, T.; Masaki, K.; Yoshida, S.: High-cycle rotating bending fatigue properties in

very long life regime of high-strength steel. *Fatigue Fract Engng Mat Struct* 2002; 25: pp. 823-30

- [8] Murakami, Y.: *Metal Fatigue: Effects of small defects and non-metallic inclusions*. Elsevier, London, 2002
- [9] Shiozawa, K.; Morii, Y.; Nishino, S.; Lu, L.: Subsurface crack initiation and propagation mechanism in high-strength steel in a very high cycle fatigue regime. In: *Intern. J. Fatigue*, Vol. 28, 2006, pp. 1521-1532
- [10] Sakai, T.; Sato, Y.; Oguma, N.: Characteristic S-N properties for high-carbon-chromium-bearing steel under axial loading in long-life fatigue. In: *FFEMS 25 (2002)* pp. 765-773
- [11] Mayer, H.: Fatigue damage of low amplitude cycle under variable amplitude loading condition. In: *Proc VHCF 4. Ann Arbor; 2007*. pp. 333-340
- [12] Mayer, H.; Stojanovic, S.; Ede, C.; Zettl, B.: Beitrag niedriger Lastamplituden zur Ermüdungsschädigung von 0,15%C Stahl. *Mat.-wiss. U. Werkstofftech.* 2007; 38, No.8
- [13] Mayer, H.; Fitzka, M.; Schuller, R.: Ultrasonic fatigue testing of 2024-T351 aluminium alloy at different load ratios under constant and variable amplitude. In: *Proc. of VHCF5, Berlin, 2011*, pp. 355-360
- [14] Mayer, H.; Haydn, W.; Schuller, R.; Issler, S.; Bacher-Höchst, M.: Very high cycle fatigue properties of bainitic high carbon-chromium steel under variable amplitude conditions, *Int. J. Fatigue* 2009; 31: pp. 1300-1308
- [15] Issler, S.; Bacher-Höchst, M.; Haydn, W.: Fatigue design for components under variable amplitude loading in the very high cycle fatigue area. In: *Sonsino, C.M.; McKeighan, P.C. (eds.): 2nd Int. Conference on Material and Component Performance under Variable Amplitude Loading, DVM, Berlin, 2009*, pp. 935-943
- [16] Nakajima, M.; Kamiya, N.; Itoga, H.; Tokaji, K.; Ko, H.: Experimental estimation of crack initiation lives and fatigue limit in subsurface fracture of a high carbon chromium steel. In: *Int. J. Fatigue*, 2006, 28 (11), pp. 1540–1546.
- [17] Lu, L.; Shiozawa, K.: Effect of two-step load variation on giga-cycle fatigue and internal crack growth behaviour of high carbon-chromium bearing steel. In: *Sakai, T.; Ochi, Y. (eds.): Proc. of VHCF3. Japan, Society of Material Science, 2004*, pp. 185-192
- [18] Mayer, H.; Fitzka, M.; Schuller, R.: Ultrasonic fatigue testing of 2024-T351 aluminium alloy at different load ratios under constant and variable amplitude. In: *Berger, C.; Christ, H.-J. (eds.): Proc. of VHCF5. DVM, Berlin, 2011*, pp. 355-360
- [19] Mayer, H.: Fatigue crack growth and threshold measurements at very high frequencies. In: *International Materials Reviews*, 1999, 44 (1), p. 1–34.
- [20] Edwards, P.R.; Darts, J. (Eds.): *Standardised Fatigue Loading Sequences for Helicopter rotors – Helix and Felix – Part 1: Background and fatigue evaluation and Part 2: Final Definition of Helix and Felix*. NLR TR 84043 U, 1984

